Current **A**pplied **S**cience and **T**echnology e-ISSN: 2586-9396

Curr. Appl. Sci. Technol. 2025, Vol. 25 (No. 5), e0263964

Research article

Improving Monitored $PM_{2.5}$ Data from Low-Cost Sensors in Chiang Mai, Thailand: Utilizing a Nonlinear Regression Modeling Approach

Natthanidnan Sricharoen[1], Titaporn Supasri[2]*, Patrinee Traisathit[3], Sukon Prasitwattanaseree[3], Pimwarat Srikummoon[3] and Jeerasak Longmali[2]

[1]Department of Statistics, Faculty of Science, Chiang Mai University, under the CMU Presidential Scholarship, Chiang Mai, Thailand
[2]National Astronomical Research Institute of Thailand, Chiang Mai, Thailand
[3]Department of Statistics, Faculty of Science, Chiang Mai University, Chiang Mai, Thailand

Received: 10 July 2024, Revised: 9 December 2024, Accepted: 10 December 2024, Published: 27 March 2025

Abstract

Air pollution, particularly particulate matter ≤ 2.5 μm ($PM_{2.5}$), is a significant global concern for human health. Technological advances in light-scattering low-cost sensors (LCSs) have facilitated extensive deployment of these devices, enhancing the spatial and temporal resolution of air quality monitoring networks beyond traditional stations. However, LCS measurements often face systematic biases and uncertainties due to technological limitations. This study aimed to calibrate LCS $PM_{2.5}$ data collected from February 14 to July 31, 2022, in Chiang Mai, Thailand, against reference measurements from the Pollution Control Department (PCD). Two nonlinear regressions, generalized additive model (GAM) and random forest (RF), were employed with linear regression (LR) as the baseline model. Model performance was evaluated using 10-fold and holdout cross-validation and metrics including R^2, RMSE, MAE, and MAPE. GAM exhibited superior performance compared to LR and RF when incorporating environmental and temporal factors such as temperature, humidity, month, and time (R^2 = 0.915, RMSE = 5.084 μg/m³). The LR model showed comparable performance (R^2 = 0.900, RMSE = 5.494 μg/m³), while RF performed well with environmental factors alone (R^2 = 0. 892, RMSE = 5.742 μg/m³). The GAM calibration significantly reduced MAPE to 17%, followed by LR (19%) and RF (21%). This study demonstrates that the integration of both environmental and temporal variables within the GAM framework is crucial for accurately calibrating LCS $PM_{2.5}$ data in northern Thailand, considering the region's distinct atmospheric characteristics. Our study underscores the necessity of including environmental and temporal factors in GAM to calibrate LCS-collected $PM_{2.5}$ data in northern Thailand.

Keywords: air quality; low-cost sensors; bias correction; nonlinear regression

*Corresponding author: E-mail: titaporn@narit.or.th
https://doi.org/10.55003/cast.2025.263964

1. Introduction

Air pollution, specifically ambient fine particulate matter with a diameter of ≤2.5 μm ($PM_{2.5}$), has become an increasingly serious global health problem that is contributing significantly to all-cause morbidity and mortality rates worldwide (Chu et al., 2020; Hua et al., 2021; McFarlane et al., 2021; Tomášková et al., 2022; Tsai et al., 2022). According to the World Health Organization, $PM_{2.5}$ causes detrimental health effects that lead to more than 7 million premature deaths annually worldwide, accounting for approximately 65% of mortality attributable to outdoor air pollution (Anderson et al., 2012; Taimuri et al., 2022; Salehi et al., 2023; World Health Organization, 2024). Over the past decade, Thailand has faced significant challenges due to high $PM_{2.5}$ levels, particularly in the northern region. These high levels are primarily a result of forest fires and the open burning of agricultural waste for land clearing and crop preparation during the dry season (January–April) (Vichit-Vadakan & Vajanapoom, 2011; Pani et al., 2019; Thepnuan et al., 2019; Dejchanchaiwong et al., 2023). In addition, transboundary pollution from neighboring countries in the Mekong Subregion (including Laos, Cambodia, Vietnam, and Myanmar) significantly contributes to air pollution in Thailand's northern and northeastern regions (Chantara et al., 2019). Consequently, it is critical to provide the public and administrative agencies with an air pollution alert system to enable individuals to take protective action by strengthening air particulate matter (PM) pollution monitoring and formulating a series of pollutant emission reduction plans.

The reference-grade air quality monitoring network in Thailand operated by the Pollution Control Department (PCD) under the Ministry of Natural Resources and Environment continuously monitors air pollutants such as dust, suspended particulate matter (PM_{10} and $PM_{2.5}$), sulfur dioxide (SO_2), carbon monoxide (CO), nitrogen dioxide (NO_2), and ground-level ozone (O_3). A filter-based inertial or gravimetric technique along with a well-constructed size-selection inlet comprising an automatic beta ray attenuation (BAM) or a tapered element oscillating microbalance (TEOM) is conventionally used as a reference method to evaluate other indirect measurement techniques. The reference technique is not strongly affected by relative humidity since the monitor contains a heated sampler inlet that reduces the moisture deposition in the system. The reference technique has been subjected to extensive field evaluation at which time the PM concentration measurements were equilibrated via the United States Federal Reference Method, thereby ensuring high accuracy and reliability (Bai et al. 2020; Raysoni et al., 2023). In Thailand, BAM or TEOM mass monitors are employed to routinely measure the hourly and daily $PM_{2.5}$ concentrations at 96 stations in 64 provinces in Thailand’s air quality monitoring network. The reference-grade air quality monitoring network can provide high temporal resolution PM measurements, yet the systems are relatively expensive and sparsely deployed at central monitoring sites in each province due to the high cost of installation and maintenance of the air quality monitoring instruments (Dejchanchaiwong et al., 2023).

One promising solution is the use of low-cost sensors (LCSs) for $PM_{2.5}$ exposure assessment to supplement the reference-grade monitoring network. LCSs can be installed in large numbers, enabling the construction of a high spatial and temporal resolution $PM_{2.5}$ network (Neal et al., 2014; Lyu et al., 2017; Hong et al., 2021; Hua et al., 2021; McFarlane et al., 2021). LCSs are typically based on optical particle counters (OPCs), which use light scattering to estimate the concentration of particulate matter. As air passes through the sensor, particles scatter light, the intensity of which is proportional to the size and number of particles present. This enables the measurement of $PM_{2.5}$ concentrations in real-time with minute-level resolution (Salimifard et al., 2019; Hagan & Kroll, 2020; Giordano et al.,

2021). While LCS monitoring is not as precise as that using reference-grade monitors, advancements in sensor technology and calibration methods have improved the accuracy and reliability of the former. Moreover, they are much cheaper than reference-grade monitors and their compactness, lightness, portability and low maintenance requirements allow for their dense deployment, significantly improving the coverage for $PM_{2.5}$ monitoring (Salimifard et al., 2019; Chu et al., 2020; Hagan & Kroll, 2020; Giordano et al., 2021; Hua et al., 2021; McFarlane et al., 2021). This approach is especially beneficial for low and middle-income countries where few, if any, reference-grade measurement devices have been deployed and in areas where the concentration fields of air pollutants have significant spatial gradients (McFarlane et al., 2021). For instance, a study conducted in Accra, Ghana highlights the challenges of quantifying air pollution exposure and its impacts due to limited access to air quality monitoring. By collocating data from a PurpleAir $PM_{2.5}$ LCS with those from a Met One Beta Attenuation Monitor 1020, this initiative represents a crucial step towards developing methods that provide high-quality, affordable, and accessible air pollution data. This is vital for communities in areas with limited access to reference-grade air pollution monitors, and thereby enabling a better understanding of and timely response to air quality issues (McFarlane et al., 2021). In Thailand, entities such as The National Astronomical Research Institute (NARIT) have exploited LCSs as part of the Air Quality Awareness Raising under the American-Thai Collaboration (AQAAT) initiative. However, the affordability and simplicity of LCSs come with a trade-off, particularly due to their reliance on light-scattering (nephelometric) principles. LCSs are inherently sensitive to the microphysical properties of aerosols; environmental factors such as aerosol size distribution, temperature, and relative humidity (RH); as well as emission sources all of which can introduce bias in the measurements (Chu et al., 2020; Hua et al., 2021; McFarlane et al., 2021, Srishti et al., 2022; Lavanyaa et al., 2022). For instance, a high RH level can cause particles to swell, leading to overestimation of the PM concentration. Moreover, the performance of LCSs also varies based on the emission source and particle characteristics such as size, shape, and refractive index (Noti et al., 2013). This variability, combined with differences in sensor model designs and the geometry of the measurement cell, can result in inconsistent readings among different sensors (Weisserta et al., 2019); this can lead to sensitivity issues that need to be addressed through careful calibration and correction strategies. Numerous researchers have pointed out the inconsistency between LCSs and high-quality regulatory instruments, with the former being relatively poor in terms of accuracy and reliability (Neal et al., 2014; Lyu et al., 2017; Hong et al., 2021; Hua et al., 2021; McFarlane et al., 2021). To provide high-quality data, the raw data need to be calibrated, and correction factors need to be developed.

Several methods have been applied to perform in-field calibrations for a variety of LCSs. The most widely used model is linear regression, in which it is assumed that there is a linear relationship between the LCS data and the reference-grade $PM_{2.5}$ measurements (McFarlane et al., 2021). Nevertheless, given the intricate nature of atmospheric chemistry, it has become imperative to employ calibration methods that can deal with nonlinear relationships (Hua et al., 2021; McFarlane et al., 2021; Lavanyaa et al., 2022; Srishti et al., 2022). For instance, RH causes particles to grow through moisture absorption as well as the formation of water droplets that can be detected as aerosols, which can cause a nonlinear relationship. Meanwhile, a secondary source of particulate matter is via photochemical reactions from precursor gases under high solar radiation, which can cause a nonlinear increase in $PM_{2.5}$ concentration (McFarlane et al., 2021; Lavanyaa et al., 2022; Srishti et al., 2022). In addition, meteorological conditions such as wind speed and direction can disperse or concentrate pollutants, thereby adding another layer of nonlinearity (Yang et al., 2021). To address these challenges, advanced calibration techniques such as

nonlinear regression models and machine-learning techniques have been adopted to better account for these variations in LCS $PM_{2.5}$ data. However, the calibration process remains complicated due to environmental factors such as RH and temperature that can affect sensor performance in unpredictable ways. Collinearity between these variables can further complicate the development of robust calibration models that perform consistently across diverse field conditions. Moreover, sensor aging causes sensitivity to drift over time, which requires frequent recalibration to maintain accuracy (Anik et al., 2021). Despite these limitations, LCSs, when effectively calibrated, remain a cost-effective and valuable tool for air quality monitoring, especially in resource-limited settings. Their ability to enhance spatial and temporal resolution makes them crucial in improving air quality surveillance where reference-grade monitoring networks are insufficient.

In the present study, we utilized two nonlinear regression approaches, a generalized additive model (GAM) and random forest (RF) and linear regression (LR) as a baseline model, to calibrate hourly $PM_{2.5}$ measurements potentially confounded by factors such as %RH and temperature with those from a standard pollution monitoring station (35T) in Chiang Mai, northern Thailand, during both the dry and rainy seasons. We sought to reduce the systematic error by elucidating the error patterns to calibrate the LCS-based $PM_{2.5}$ data. This $PM_{2.5}$ data supplementation approach may provide better support for dynamic air quality management practices.

2. Materials and Methods

2.1 Data sources

The LCSs used in this research employing a light-scattering technique to measure real-time PM concentrations were acquired under the AQAAT project. LCS $PM_{2.5}$ data collection was carried out during the dry and rainy seasons in Chiang Mai, Thailand. The dry season is marked by high $PM_{2.5}$ concentrations due to both domestic sources, particularly forest fires and agricultural waste burning, and transboundary sources from neighboring countries. In contrast, the rainy season is characterized by high humidity, which can affect the accuracy of LCS readings. Details about the low-cost LCSs used in this research can be found at https://aqaat.narit.or.th/aqaat/index.php.

The $PM_{2.5}$ data from LCSs located approximately 4 km away from a reference PCD monitoring station, located at 18.85296 N latitude and 98.95763 W longitude, in Chiang Mai (PCD station#35T/CM) were acquired from February 14, 2022, to July 31, 2022. Hourly aggregated $PM_{2.5}$ data from both the reference and LCS sensors, as well as the RH and temperature levels, were used in the analysis. To justify the acceptability of the 4 km distance between the LCS and the reference monitoring station, we conducted an additional analysis comparing $PM_{2.5}$ concentrations between two standard PCD monitoring stations in Chiang Mai (Stations 35T and 36T), which are approximately 6-7 km apart. The comparison showed that the $PM_{2.5}$ concentrations at these two stations were highly consistent, with minimal differences (Table 1 and Figures 1 and 2). This suggests that $PM_{2.5}$ concentrations are relatively uniform over distances up to 7 km in our study area, supporting the acceptability of the 4 km separation between our LCS and PCD Station 35T. Similar to the EPA's Air Sensor Guidebook, it indicated that this proximity was sufficient for comparative monitoring while reflecting local microenvironmental conditions. Moreover, distances of between 1 and 5 km have been employed in similar studies (Wang et al., 2020; Margaritis et al., 2021; Jon et al., 2023), which the author posited ensured spatial

Table 1. Statistical summary of the $PM_{2.5}$ of two reference-grade monitoring from February 14, 2022 to July 31, 2022

Reference Measurements	Mean ± SD (µg/m³)	Range (µg/m³)	Mean Difference (µg/m³)	95% Limits of Agreement (µg/m³)
PCD Station 35T	27.03±16.47	7.52 – 73.65	0.0067	-0.6436 – 0.6570
PCD Station 36T	27.02±16.44	7.45 – 72.21		

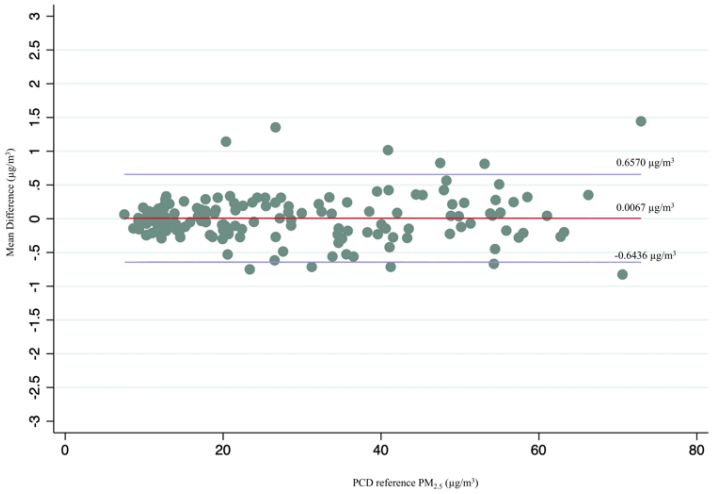

Figure 1. Bland-Altman analysis

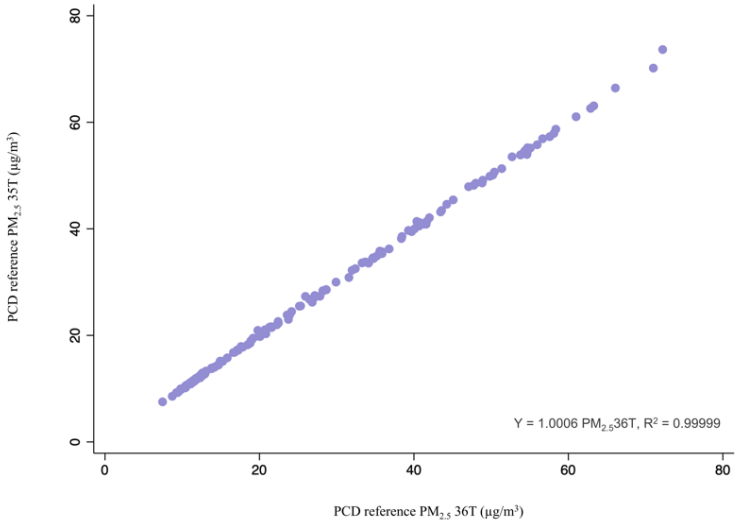

Figure 2. Scatter plot between two reference-grade monitoring (PCD Station 35T and 36T)

representativeness and could account for variability in pollution sources. Thus, the distance between the sensors in our study ensures that the LCS readings encompass local atmospheric conditions while still allowing for effective comparison with the reference station, thus providing a more comprehensive assessment of $PM_{2.5}$ levels in the region.

2.2 Variables selection

In developing the calibration equations for the LCS, we employed a forward stepwise regression approach for variable selection. This method was chosen due to its efficiency in identifying a subset of predictors that significantly contribute to the model while minimizing multicollinearity and overfitting. The process begins with an empty model and sequentially adds predictors by adding one variable at a time based on its contribution to the model's performance. This is specifically assessed through improvements in the coefficient of determination (R^2) (McFarlane et al., 2021). Their statistical significance is also assessed using p-values and Akaike Information Criterion (AIC) results for model evaluation. Table 2 illustrates the variable selection for each calibration method. Several studies have demonstrated the efficacy of forward stepwise regression in the calibration of air quality models. For instance, in the work of McFarlane et al. (2021) on calibrating low-cost air quality sensors, forward selection was used to enhance model accuracy by systematically including significant predictors while avoiding overfitting. Furthermore, the process of selecting variables was conducted iteratively. Although increasing the number of input variables can improve the R^2 value for the model, adding redundant variables with minimal contributions to R^2 can result in collinearity issues. Thereby, we sought the optimal balance between predictive accuracy and model simplicity.

Table 2. The LR, GAM and RF models used to calibrate the LCS-derived $PM_{2.5}$ concentration data

Model	Type	Equations
1	LR	$PM_{2.5,\,ref} = f(PM_{2.5,\,LCS})$
2	LR	$PM_{2.5,\,ref} = f(PM_{2.5,\,LCS} + Temp_{LCS})$
3	LR	$PM_{2.5,\,ref} = f(PM_{2.5,\,LCS} + Temp_{LCS} + RH_{LCS})$
4	LR	$PM_{2.5,\,ref} = f(PM_{2.5,\,LCS} + Temp_{LCS} + RH_{LCS} + Month)$
5	LR	$PM_{2.5,\,ref} = f(PM_{2.5,\,LCS} + Temp_{LCS} + RH_{LCS} + Month + Time)$
6	GAM	$PM_{2.5,\,ref} = s(PM_{2.5,\,LCS})$
7	GAM	$PM_{2.5,\,ref} = s(PM_{2.5,\,LCS}) + s(Temp_{LCS})$
8	GAM	$PM_{2.5,\,ref} = s(PM_{2.5,\,LCS}) + s(Temp_{LCS}) + s(RH_{LCS})$
9	GAM	$PM_{2.5,\,ref} = s(PM_{2.5,\,LCS}) + s(Temp_{LCS}) + s(RH_{LCS}) + f(Month)$
10	GAM	$PM_{2.5,\,ref} = s(PM_{2.5,\,LCS}) + s(Temp_{LCS}) + s(RH_{LCS}) + f(Month) + f(Time)$
11	RF	RF model with $PM_{2.5,LCS}$
12	RF	RF model with multiplicative terms $PM_{2.5,LCS}$, and $Temp_{LCS}$
13	RF	RF model with multiplicative terms $PM_{2.5,LCS}$, $Temp_{LCS}$, and RH_{LCS}
14	RF	RF model with multiplicative terms $PM_{2.5,LCS}$, $Temp_{LCS}$, RH_{LCS}, and month
15	RF	RF model with multiplicative terms $PM_{2.5,LCS}$, RH_{LCS}, $Temp_{LCS}$, and time

2.3 Calibration models

Hourly $PM_{2.5}$ concentration data from LCSs were constrained between 0 μg/m^3, and 1000 μg/m^3, with RH level restricted to greater than 0%. Three different models were tested for their ability to correct low-cost sensor data: linear regression, generalized additive model, and random forest. Following the feature selection process, each calibration model utilized three primary parameters from the LCS as explanatory variables: the LCS-derived $PM_{2.5}$ concentration, temperature (T, °C), and RH (%), and two temporal features (month and time of day). The calibrated models used $PM_{2.5}$ concentration from PCD station#35T/CM as the dependent variable, represented as follows:

$$PM_{2.5}[Ref] = f(PM_{2.5}[LCS],\ T[LCS],\ RH[LCS],\ Month[Derived],\ Time[Derived]) \quad (1)$$

where $PM_{2.5}[Ref]$ is $PM_{2.5}$ concentration from PCD station#35T/CM, $PM_{2.5}[LCS]$ represent the LCS $PM_{2.5}$ concentration, T is the temperature recorded by LCS $PM_{2.5}$ monitor, and RH is the relative humidity recorded by LCS $PM_{2.5}$ monitor. The month was derived was derived from the timestamp of the collected data, and time of day was categorized into four groups: morning (6:00 AM – 10:00 AM), noon (11:00 AM – 4:00 PM), evening (5:00 PM – 8:00 PM), and night (9:00 PM – 5:00 AM).

2.3.1 LR

LR was employed as the baseline model to optimize the best fit by minimizing the distance between the observed values (i.e., reference-grade $PM_{2.5}$ concentrations) and the predicted values (LCS $PM_{2.5}$ corrected). LR is advantageous due to its simplicity, ease of interpretation, and ability to facilitate using a standard equation. Linear and higher-order polynomial fits are among the least computationally demanding methods and are easy to implement, making them the most commonly utilized correction techniques in the calibration of low-cost sensors (Wang et al., 2020). The linear regression approach followed the structure outlined in equation (2).

$$PM_{2.5,ref} = \beta_0 + \sum_{i=1}^{n} f_i(x_i) + \varepsilon, \quad (2)$$

where β_0 represents the intercept, x_i denotes a set of predictors (LCS $PM_{2.5}$, temperature, RH, month, and time of day), n is the number of selected predictors, and ε represents the residual.

2.3.2 GAM

GAM was employed as a nonlinear regression method between predictors and the response variable, the framework for which is

$$PM_{2.5,ref} = \beta_0 + \sum_{i=1}^{n} s_i(x_i) + \varepsilon, \quad (3)$$

where β_0 represents the intercept for GAM, and x_i denotes a set of predictors (LCS $PM_{2.5}$, temperature, RH, month, and time). $s(\cdot)$ refers to the P-spline smoothing functions, which optimize the model fit and control the smoothness through a penalty term (Hastie &

Tibshirani, 1986; Eilers & Marx, 1996), the smoothers of $s_i(x_i)$ characterize the effects of the predictors on the reference $PM_{2.5}$ concentrations, n is the number of selected predictors, and ε represents the residual.

2.3.3 RF

This is a machine-learning algorithm designed to address regression or classification tasks (Raheja et al., 2023). It operates by constructing a supervised ensemble of decision trees that individually isolate errors within a training dataset. The collective prediction from this ensemble (typically the mean value across the decision trees) is subsequently utilized for predicting outcomes based on new input data (Raheja et al., 2023). In the context of LCS $PM_{2.5}$ concentration analysis, calibrating the RF model necessitates adjusting its hyperparameters. To optimize the model performance, a grid search was conducted using the 10-fold cross-validation technique and employing the coefficient of determination (R^2) metric for evaluation.

2.4 Performance metrics

We conducted both 10-fold cross-validation and holdout validation tests to evaluate the robustness of the models and to mitigate overfitting, thereby ensuring that the method performed reliably on unseen data. We also applied residual diagnostics using the Durbin-Watson statistic to assess autocorrelation: values near 2 indicate minimal autocorrelation, thus supporting the independence assumption for residuals. When significant autocorrelation was observed, adjustments were made using lagged variables to enhance the model performance. The performance of the calibration models were assessed using several metrics: R^2, the root-mean-square error (RMSE), the mean absolute error (MAE), and the mean absolute percentage error (MAPE). The R^2 metric, with values ranging between 0 and 1, was used to quantify the degree of correlation between the calibrated LCS and reference $PM_{2.5}$ values: the value closest to 1 indicates the best fit. RMSE measures the average magnitude of the errors between the calibrated LCS and reference $PM_{2.5}$ values, with the lowest value indicating the best performance. MAE and MAPE were used to assess any discrepancies between the LCS and reference $PM_{2.5}$ values (Wang et al., 2020; Srishti et al., 2022). These metrics are defined as follows:

$$R^2 = 1 - \frac{\sum_{i=1}^{n}(y_i - \hat{y}_i)^2}{\sum_{i=1}^{n}(y_i - \bar{y})^2}, \tag{4}$$

$$RMSE = \sqrt{\frac{\sum_{i=1}^{n}(y_i - \hat{y}_i)^2}{n}}, \tag{5}$$

$$MAE = \frac{1}{n}\sum_{i=1}^{n}|y_i - \hat{y}_i|, \tag{6}$$

$$MAPE = \frac{1}{n}\sum_{i=1}^{n}\left|\frac{y_i - \hat{y}_i}{y_i}\right| \times 100, \tag{7}$$

where $\hat{y}_i$ represents the calibrated values of LCS $PM_{2.5}$, y_i denotes the reference $PM_{2.5}$ values, $\bar{y}$ is the average concentration of reference $PM_{2.5}$, and n is the number of measurements. Data preprocessing, data analysis, LR, GAM and RF calculation, and

model validation process were conducted using the R environment (Version 4.3.3) leveraging packages including “gam,” “ggplot2,” “mgcv,” “tidyr”, “plotly”, “dplyr”, “caret”, “randomForest” and “car”.

3. Results and Discussion

3.1 Measurements of LCS and reference-grade monitoring

The hourly averaged LCS and reference $PM_{2.5}$ concentration, RH, and temperature data from February 14, 2022, to July 31, 2022, obtained at NARIT site Chiang Mai-35T are summarized in Table 3. During the dry season, the $PM_{2.5}$ concentration reached 96 $\mu g/m^3$ (based on the reference data) and 148 $\mu g/m^3$ (based on the LCS data). The overall-averaged $PM_{2.5}$ concentration during the dry season using the LCS measurements was 43.4±21.8 $\mu g/m^3$, approximately three times higher than the overall-averaged $PM_{2.5}$ concentration during the rainy season (11.3±8.4 $\mu g/m^3$). Contrastively, these were 37.7±16.7 and 14.6±6.2 $\mu g/m^3$, respectively, using the reference data. Our findings align with those from a previous study (Jainontee et al., 2023). The primary contributors to air pollution in Chiang Mai are domestic activities such as forest fires and agricultural waste burning during the dry season. This is due to Chiang Mai's geography, featuring high mountains along the north-south corridor with significant forest and agricultural coverage (Dejchanchaiwong et al., 2023). In addition, aerosol transport from biomass burning in parts of Myanmar and Laos also impacts the air quality in northern Thailand (Chantara et al., 2019). From the LCS measurements, the average RH and temperature during the dry season ranged from 25-86% and 20.8-35.7°C, respectively, and the RH was 5-25% higher and the temperature was slightly higher during the rainy season. Increased RH levels may cause particle swelling, leading to an overestimation of PM concentrations.

Table 3. Statistical summary of the $PM_{2.5}$ measurement parameters by season from February 14, 2022, to July 31, 2022

Season	Parameter	Unit	Reference Measurements		LCS Measurements	
			Mean±SD	Range	Mean±SD	Range
Dry						
	$PM_{2.5}$	$\mu g/m^3$	37.7±16.7	3.0 – 96.0	43.4±21.8	1.0 – 148.0
	T	C	27.6±4.4	17.0 – 39.1	28.6±2.9	20.8 – 35.7
	RH	%	60.8±18.7	18.0 – 99.0	58.6±12.2	25.0 – 86.0
Rainy						
	$PM_{2.5}$	$\mu g/m^3$	14.6±6.2	3.0 – 58.0	11.3±8.4	0.0 – 24.8
	T	C	27.3±3.2	21.7 – 37.6	28.0±1.9	24.8 – 34.2
	RH	%	76.1±16.3	37.0 – 99.0	75.1±9.2	47.0 – 91.0

Figure 3 illustrates the seasonal variation in the 24-hour-average $PM_{2.5}$ concentration measured using the LCS and reference monitor. Overall, the uncalibrated LCS measurements generally followed the trend observed in the reference measurements.

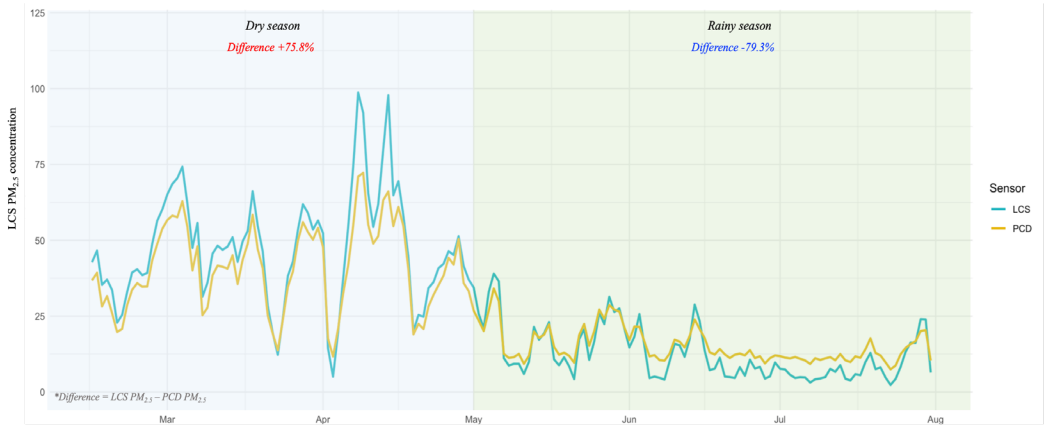

Figure 3. Twenty-four-hour average $PM_{2.5}$ concentrations measured using the reference monitor (PCD) and the LCS from February 14, 2022, to July 31, 2022, in Chiang Mai, Thailand

Notably, during the hottest month of the year in Thailand (April), the uncalibrated LCS $PM_{2.5}$ concentrations were approximately 1.5 times higher than those recorded using the reference-grade monitor. Many low-cost sensors tend to saturate at high $PM_{2.5}$ concentrations, typically above 100 μg/m³, leading to overestimated readings. This limitation in sensor design prevents accurate measurement during severe pollution episodes, resulting in inflated concentration values (Dejchanchaiwong et al., 2023). This finding is consistent with a previous study in Wenshang County, Shandong Province, China (Hua et al., 2021), the authors of which reported that LCSs overestimated $PM_{2.5}$ concentrations by approximately 1.4 times in dry conditions and 2.0 times in humid conditions compared to a reference monitor. In contrast, our findings showed that LCS $PM_{2.5}$ concentrations were consistently underestimated by approximately 2 times during the rainy season, particularly in June and July, when heavy rainfall occurred in Chiang Mai. This result contradicts the expected behavior of LCSs, which generally overestimate concentrations at high RH levels due to particle swelling. The unexpected underestimation observed in our study could be attributed to limitations in the sensor's response mechanism under high humidity conditions, which may have caused interference in the sensor's ability to accurately detect PM concentrations. Another possible explanation for this underestimation is the condensation effect, where the accumulation of moisture on the sensor surface might have reduced the efficiency of particle detection, leading to lower readings (Park et al., 2021). In our study, $PM_{2.5}$ concentrations measured using LCSs were found to be 75.8% higher than those measured by reference instruments during the dry season. This finding aligns with (Dejchanchaiwong et al., 2023), who reported that the Plantower LCS overestimated $PM_{2.5}$ concentrations in Chiang Mai, which reached 246 $\mu g/m^3/d$ during the dry season. However, we also observed that RH significantly influenced LCS particulate matter measurements performance. Under high RH conditions, the LCS tended to underestimate the actual values from May to August (the rainy season) (79.3% lower). LCS devices are known to be highly sensitive to RH, and numerous studies have shown that LCS performance deteriorates with low $PM_{2.5}$ concentrations and high RH (Hua et al., 2021). Similarly, Jayaratne et al. (2018) found that $PM_{2.5}$ concentrations reported by an LCS increased exponentially with RH up to 75%. These findings highlight the importance of calibrating LCSs for different environmental conditions, such as high-

humidity conditions during the rainy season in tropical regions. In addition, our results align with findings from other countries, such as the United States (Sousan et al., 2016), where it was observed that LCS devices respond differently depending on the climate conditions. It has been recommended that calibration is performed under specific conditions to minimize errors (Nalakurthi et al., 2024). Thus, RH can significantly impact the accuracy of $PM_{2.5}$ concentration measurements using LCSs.

The linear regression R^2 value used for comparing the $PM_{2.5}$ concentration data from the LCS and reference monitor was notably high (0.947) (Figure 4). A slope value significantly deviating from 1 indicates that potential systematic bias or inconsistency in measurements caused by variations in humidity and temperature and/or interference from other particulate matter such as dust or pollen can skew the results, particularly during high-concentration events (Jayaratne et al., 2018). Notably, some extreme values were observed when the $PM_{2.5}$ concentration exceeded 70 $\mu g/m^3$, resulting in an unstructured pattern. This anomaly can be attributed to the significant air pollution contribution from biomass burning during the dry season (Chantara et al., 2019; Pani et al., 2019; Thepnuan et al., 2019; Dejchanchaiwong et al., 2023). However, the source contribution is not the only factor affecting measurement error. The performance of the LCS can also vary at lower $PM_{2.5}$ concentration levels. For instance, measurements below 15 $\mu g/m^3$ may exhibit greater relative error due to the sensors' inherent limitations in sensitivity and accuracy at lower concentrations. In addition, the response time of the LCS can lead to discrepancies during rapid changes in $PM_{2.5}$ levels, particularly during episodes of high pollution (Jayaratne et al., 2020). A previous study on calibrated LCS $PM_{2.5}$ data from three different locations in Thailand revealed that the LCS response varied depending on the type of aerosols (Dejchanchaiwong et al., 2023). Specifically, LCSs were more responsive to emissions from open biomass burning than to traffic emissions in large cities such as Bangkok. Moreover, the particle size from biomass burning predominantly ranges from 0.5-2.5 µm (Samae et al., 2021) or 0.5-1.0 µm in accumulation mode (Hata et al., 2014). Thus, the overestimation of $PM_{2.5}$ concentration by the LCS could be due to its heightened sensitivity to biomass burning emissions.

3.2 Feature selection for the correction models

Table 4 demonstrates the feature selection process to determine the optimal calibration models for LR, GAM, and RF. This process involved evaluating five different sets of predictors for each method. For LR, the model with the lowest AIC and the highest performance metrics was LR5, which included the following predictors: LCS $PM_{2.5}$, temperature, relative humidity, month, and time. Therefore, LR5 was selected as the final model for multiple linear regression (MLR) calibration. Similarly, for GAM, the model with the lowest AIC, highest R^2, and lowest RMSE was GAM5, which also included all five predictors (LCS $PM_{2.5}$, temperature, relative humidity, month, and time), making it the best choice for calibration. In contrast, for RF, the model with three predictors (LCS $PM_{2.5}$, temperature, and relative humidity) exhibited the most favorable performance metrics, as RF4 and RF5 showed slightly increased AIC and RMSE values. Consequently, RF3 was selected as the final calibration model for the random forest method. These selected models, LR5, GAM5, and RF3, provided the best balance between predictive accuracy and model complexity. Moreover, a significant interaction between the factors was not found (Table 5).

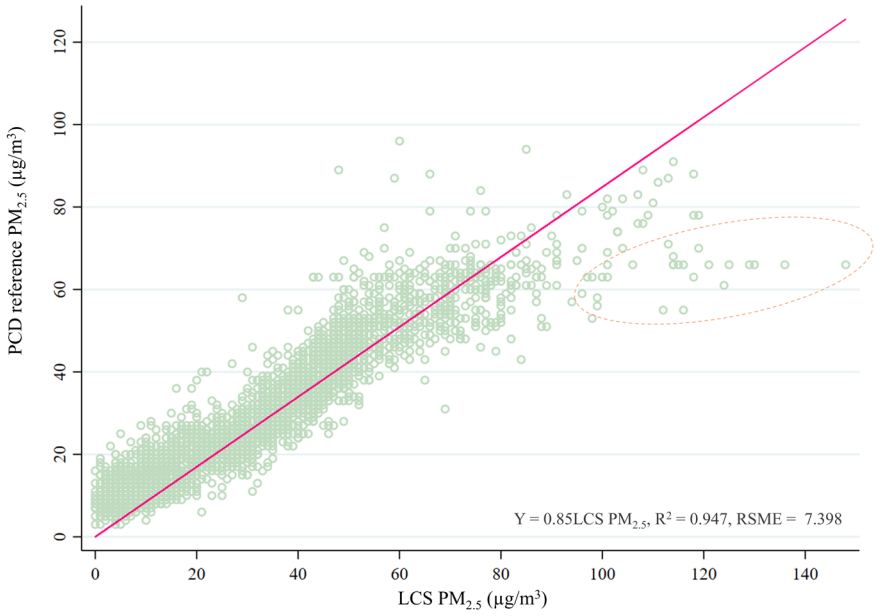

Figure 4. Hourly $PM_{2.5}$ concentration measurements by the LCS and reference monitor from the PCD. The solid line is for slope = 1 while the dashed circle highlights the extreme values.

Table 4. Feature selection for calibration models (LR, GAM, RF)

Model	Predictor(s)	AIC	R^2
LR1	LCS $PM_{2.5}$	24136.75	0.886
LR2	LCS $PM_{2.5}$; Temperature	23871.02	0.894
LR3	LCS $PM_{2.5}$; Temperature; Relative humidity	23713.99	0.898
LR4	LCS $PM_{2.5}$; Temperature; Relative humidity; Month	23664.64	0.899
LR5	LCS $PM_{2.5}$; Temperature; Relative humidity; Month; Time	23591.78	0.901
GAM1	LCS $PM_{2.5}$	23235.34	0.910
GAM2	LCS $PM_{2.5}$; Temperature	22961.99	0.917
GAM3	LCS $PM_{2.5}$; Temperature; Relative humidity	22899.46	0.918
GAM4	LCS $PM_{2.5}$; Temperature; Relative humidity; Month	22873.51	0.919
GAM5	LCS $PM_{2.5}$; Temperature; Relative humidity; Month; Time	22809.23	0.920
RF1	LCS $PM_{2.5}$	13652.13	0.906
RF2	LCS $PM_{2.5}$; Temperature	13531.94	0.909
RF3	LCS $PM_{2.5}$; Temperature; Relative humidity	13420.21	0.911
RF4	LCS $PM_{2.5}$; Temperature; Relative humidity; Month	13503.25	0.910
RF5	LCS $PM_{2.5}$; Temperature; Relative humidity; Time	14191.42	0.891

Table 5. Assessment of potential interaction between factors

Variables	*p*	Conclusion[a]
LCS $PM_{2.5}$ x Temperature		No interaction
LCS $PM_{2.5}$	<0.001	
Temperature	0.379	
Interaction	<0.001	
LCS $PM_{2.5}$ x Relative humidity		No interaction
LCS $PM_{2.5}$	<0.001	
Relative humidity	0.232	
Interaction	<0.001	
Temperature x Relative humidity		No interaction
Temperature	0.023	
Relative humidity	0.181	
Interaction	0.116	

[a]Interaction was considered significant when p-values of all terms were significant

3.3 Performance evaluation of the correction models

The robustness of the selected calibration models was evaluated through 10-fold cross-validation and holdout validation. The results of the 10-fold cross-validation for the selected MLR, GAM, and RF models were derived from the same training-validation datasets. The average RMSE and R^2 values for the three models obtained from the 10-fold cross-validation were 5.494 μg/m³ and 0.900 for MLR, 5.084 μg/m³ and 0.915 for GAM, and 5.742 μg/m³ and 0.892 for RF, respectively (Table 6).

Table 6. Comparison of model fitting and 10-fold cross-validation for hourly $PM_{2.5}$ concentrations calibrated using selected LR, GAM, and RF models

Model	R^2	RMSE (μg/m³)	MAE (μg/m³)	MAPE (%)
LR5	0.900	5.494	3.960	18.29
GAM5	0.915	5.084	3.701	17.13
RF3	0.892	5.742	4.223	20.78

The results of the holdout validation are presented in Figure 5. The differences in RMSE between the 10-fold cross-validation and the holdout validation were approximately 0.136, 0.257, and 0.317 μg/m³ for MLR, GAM, and RF, respectively. Figure 5a-f illustrates the relationships between the reference $PM_{2.5}$ measurements and the calibrated LCS output for the training and validation sets using the three correction models.

The R^2 values for the models trained using 2044 data points from the training set ranged from 0.970 to 0.976, thus indicating strong explanatory power for all three models. In terms of RMSE, GAM exhibited the lowest value (5.011 μg/m³) with the training set (Figures 5a, 5c, and 5e). A validation set of 1052 data points was used to further assess the performance of these models on new data (Figures 5b, 5d, and 5f) This time, the R^2 values for all three models ranged from 0.963 to 0.972 (thus once again indicating strong explanatory power), and the lowest RMSE value (5.341 μg/m³) was attained with GAM. In conclusion, the RMSE values for GAM were found to be 9% and 11% lower than those for MLR and RF in the training sets, and 6% and 15% in validation sets, respectively, thus indicating that GAM outperformed the other two models in terms of predictive accuracy.

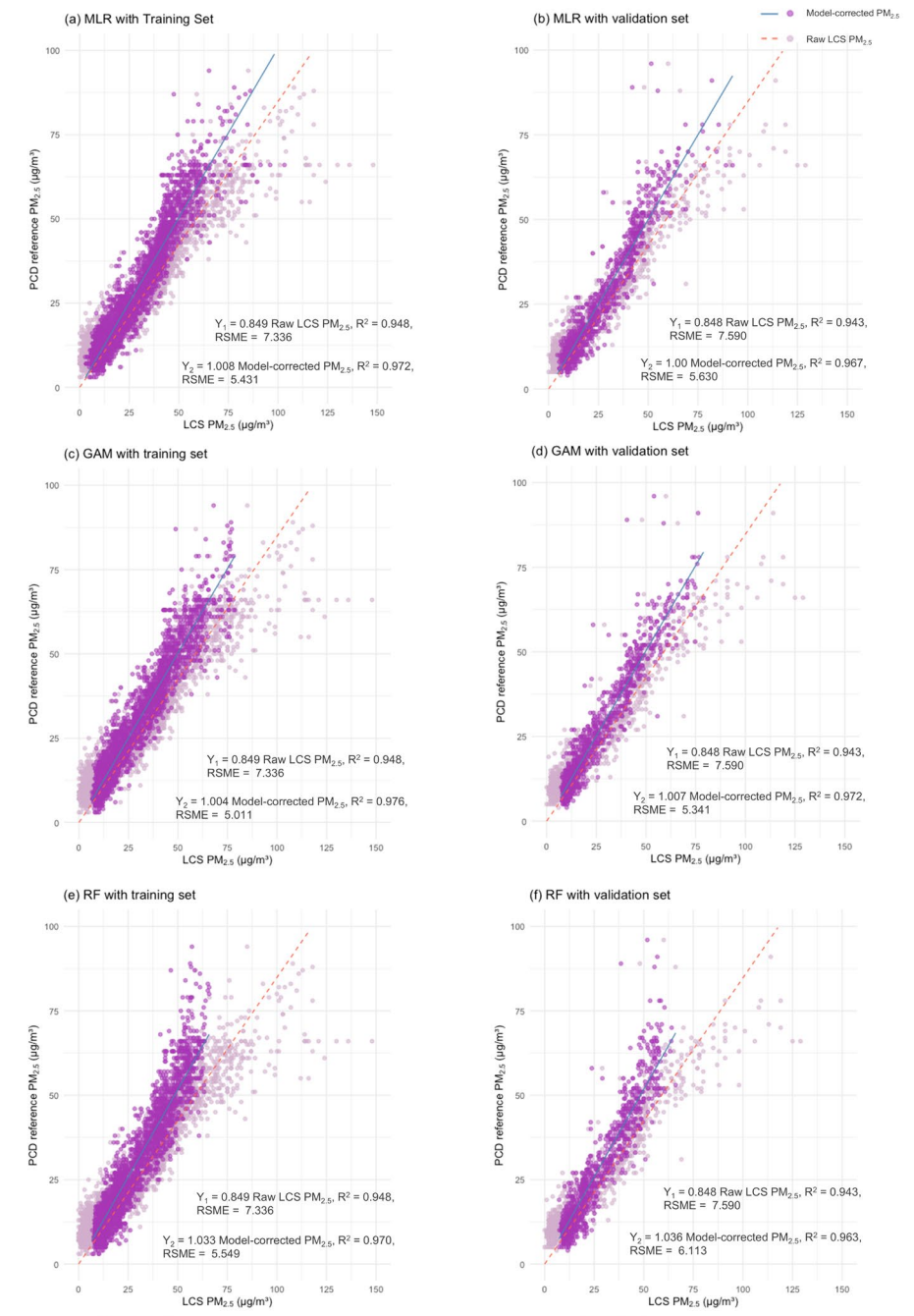

Figure 5. Model performance of (a) multiple linear regression (MLR) with training data, (b) MLR with validation data, (c) generalized additive model (GAM) with training data, (d) GAM with validation data, (e) random forest (RF) with training data, and (f) RF with validation data. The RMSE, R^2, and n are listed in the graphs.

Overall, the uncalibrated LCS $PM_{2.5}$ measurements exhibited good agreement with the corresponding measurements from the reference monitor (R^2 = 0.947) (Figure 3). Both the MLR and GAM approaches outperformed the RF model, likely due to the inclusion of environmental and temporal variables in the former two. The RF approach appears to be limited when applied to data beyond the range of the training set, which is a common limitation of tree-based algorithms (Dejchanchaiwong et al., 2023). Moreover, the R^2 values for the GAM model improved significantly with the inclusion of environmental factors such as RH and temperature, and temporal factors (monthly in this case). The integration of both meteorological and chemical parameters resulted in calibrated LCS $PM_{2.5}$ concentrations that more closely matched the reference $PM_{2.5}$ measurements (Hua et al., 2021). This is consistent with the findings of Jain et al. (2023), who reported daily-averaged $PM_{2.5}$ concentrations ranging from 4-75 μg/m³ (mean = 12.0 μg/m³), with weekend concentrations being approximately 10% higher than weekday concentrations. These results indicate that including temporal valuation, such as the time of day, can further enhance model performance. In contrast to previous studies where RF demonstrated superior performance to MLR and supported vector regression (SVR). Compared to SVR, the RMSE values of RF were 35% and 85% lower for both the training and validation sets, respectively (Wang et al., 2020). Notably, unlike our model, a temporal factor was not included in the aforementioned study. This discrepancy could be due to the larger datasets utilized in previous studies, which could have facilitated better model training and enhanced prediction accuracy compared to the present study. Among the few in-field correction studies, one research group employed a similar GAM model to correct LCS data from three Taiwan EPA stations in December 2017, and after applying the correction, the RMSE values decreased from 15.55-31.34 μg/m³ to 4.88-9.66 μg/m³ (Lee et al., 2019). These findings are comparable to our studies, which was a reduction in RMSE from 7.398 μg/m³ to 5.084 μg/m³ (Table 6).

3.4 $PM_{2.5}$ corrections

Figure 6 illustrates the reduction in the percentage of overestimated $PM_{2.5}$ values (exceeding 10 μg/m³) by the LCS after applying the LR, GAM, and RF models, decreasing from 12.3% to 3.7%, 1.7%, and 1.8%, respectively. Similarly, the percentage of underestimated $PM_{2.5}$ values (exceeding 10 μg/m³) decreased from 5.2% to 2.2%, 3.3%, and increased to 5.5%, respectively. These results suggest that the GAM model is particularly effective in mitigating overestimation at high $PM_{2.5}$ levels, while the RF model performs well in addressing underestimation at low $PM_{2.5}$ levels. These findings contrast with previous research (Hua et al., 2021), which indicated that the GAM model performed well in conditions of high RH and low $PM_{2.5}$ concentrations. In addition, it is possible that the types and characteristics of aerosols present in the study area influenced the calibration performance (Dejchanchaiwong et al., 2023). Figure 7 presents a time series plot comparing raw LCS $PM_{2.5}$ values with the model-corrected $PM_{2.5}$ values using MLR, GAM, and RF for the first half of 2022. Following calibration using observations from nearby PCD stations (35T/CM), the GAM-corrected $PM_{2.5}$ levels closely aligned with those from reference-grade monitors, significantly reducing the overestimation observed in the raw $PM_{2.5}$ measurements. However, discrepancies persisted during periods of very high $PM_{2.5}$ concentrations (April), and corrections during the rainy season exhibited greater variability, which may be attributed to the influence of RH. Similarly, the MLR model demonstrated performance comparable to GAM but exhibited higher errors during extreme $PM_{2.5}$ events.

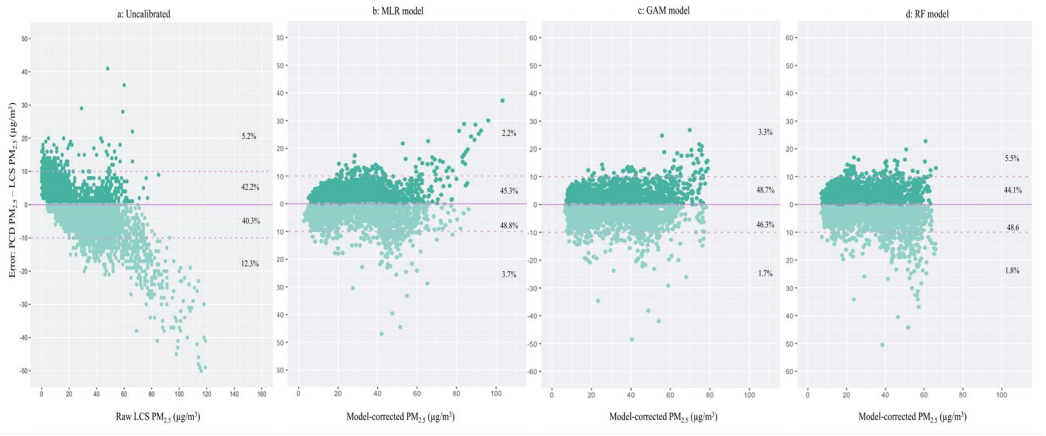

Figure 6. Error distributions of the LCS $PM_{2.5}$ data: (a) uncalibrated, (b) after MLR calibration, (c) after GAM calibration, and (d) after RF calibration

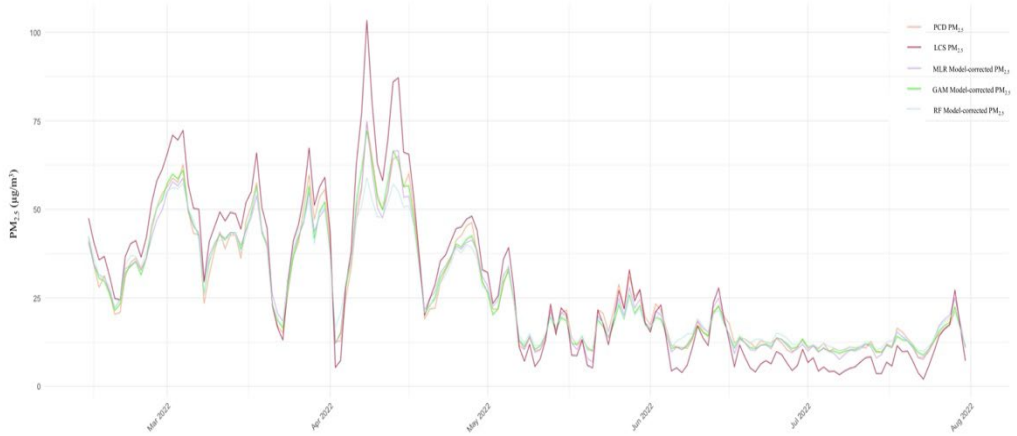

Figure 7. Time-Series of raw $PM_{2.5}$, reference-grade monitoring, and model-corrected $PM_{2.5}$ using the MLR, GAM, and RF models

In contrast, the RF model performed effectively during lower $PM_{2.5}$ levels (range 10-40 µg/m³). Normal Q-Q plots showed that residuals deviated from normality, suggesting that parametric models like MLR may not adequately capture extreme $PM_{2.5}$ events. Non-linear regression or machine learning models are recommended to improve model accuracy (Figure 8). In addition, the Durbin-Watson test results (Table 7) indicate positive autocorrelation in MLR residuals, violating the independence assumption, whereas GAM showed better adherence. These findings support exploring non-linear or machine learning approaches to improve model robustness and accuracy.

a) Linear Regression

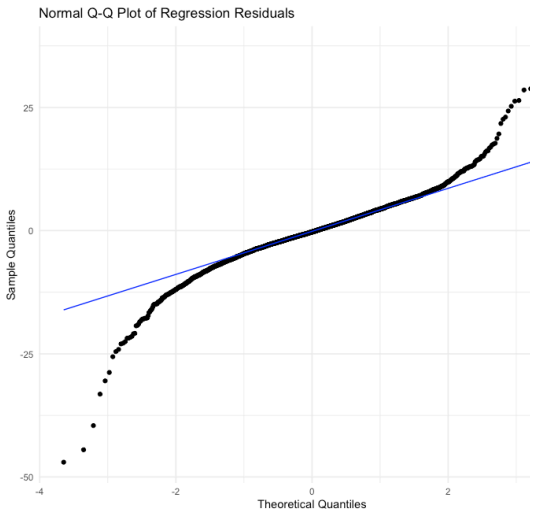

b) Generalized Additive Model

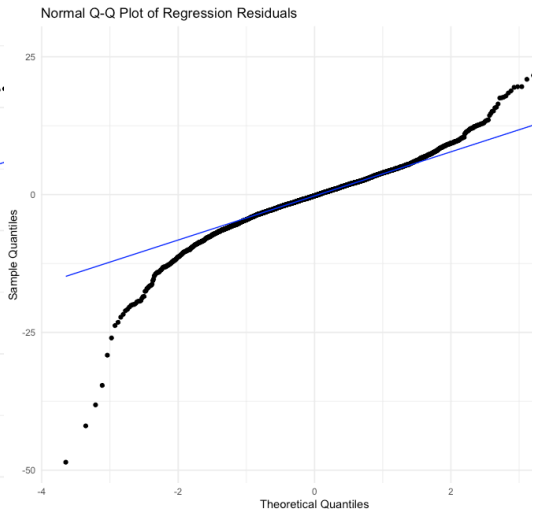

c) Random Forest

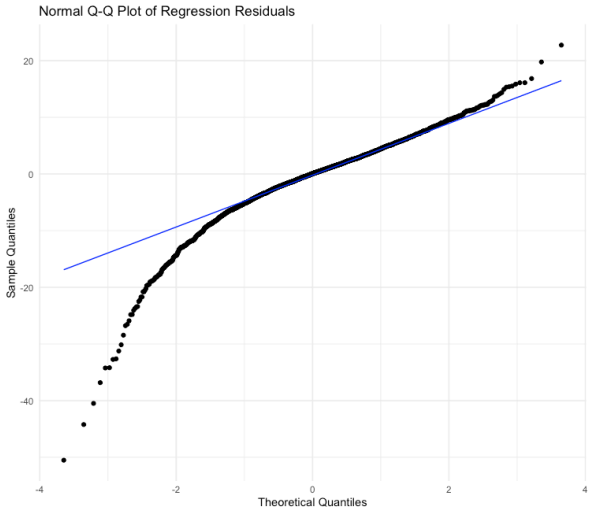

Figure 8. Normal Q-Q Plot

Table 7. Durbin-Watson test result

Model	Iteration	D-W Statistic
LR	1	1.58
LR	2	1.83
LR	3	1.61
LR	4	1.55
LR	5	1.52
LR	6	1.69
LR	7	1.78
LR	8	1.77
LR	9	1.70
LR	10	1.69
GAM	1	1.84
GAM	2	1.92
GAM	3	1.85
GAM	4	1.66
GAM	5	1.90
GAM	6	1.88
GAM	7	1.91
GAM	8	1.91
GAM	9	2.13
GAM	10	1.75

Abbreviations: LR, linear regression; GAM, generalized additive model

3.5 Limitations of this work

This study has several limitations that should be acknowledged. A more comprehensive understanding of the correction factors and their respective characteristics is necessary. Specifically, stratifying the data by season to examine the influence of each factor on the model could provide valuable insights. However, our attempt at seasonal analysis resulted in decreased model performance, which can be attributed to the relatively small dataset and data being collected from a single station over 6-months. This likely affected the model's capacity and made generalization of the findings over a longer time period impossible. Therefore, we will consider incorporating data spanning multiple years collected from multiple LCS stations to develop a more robust calibration model that can deal with temporospatial variability in the future.

Although the calibrated models significantly improved data accuracy, potential deviations could still arise from the inherent differences between ambient and street-level $PM_{2.5}$ concentrations. Street-level $PM_{2.5}$ monitoring can be influenced by various local emission sources, such as from vehicles and agricultural burning, while reference-grade monitoring stations are designed to measure well-mixed ambient $PM_{2.5}$ concentrations free from direct local emission interference. In this study, the LCS station was located within a 4 km radius of the reference-grade monitoring station and we assumed that $PM_{2.5}$ particles were uniformly distributed within this distance. However, spatial variability in the emissions

data could have made this assumption moot. In scenarios where LCS co-location with reference-grade monitoring is not feasible, alternative approaches such as employing spatial interpolation methods, such as kriging or inverse distance weighting, could be considered to estimate $PM_{2.5}$ concentrations at unsampled locations, accounting for spatial variability. In our study, we provide a practical and resource-efficient approach for calibrating LCS data without the need for exact co-location or extensive spatial interpolation, by demonstrating that $PM_{2.5}$ concentrations are relatively uniform over distances up to 7 km. This is particularly beneficial in areas where resources for establishing extensive monitoring networks are limited.

These findings underscore the importance of establishing a more extensive network of LCS stations to assess local ambient air quality comprehensively. Future research should consider co-locating LCSs with reference-grade stations when possible to facilitate direct comparisons under identical environmental conditions, thereby improving calibration accuracy and reducing potential bias. In addition, a systematic sensitivity analysis could be conducted to assess the influence of various factors, such as local emission source intensity, topographic conditions, prevailing meteorological parameters (e.g., wind speed and direction), and background pollution levels, on the spatial distribution of $PM_{2.5}$ and the reliability of assumptions about uniform pollutant dispersion. This would help identify conditions under which co-location or advanced spatial interpolation methods are essential, thereby informing the design and implementation of more effective LCS-based air quality monitoring programs. Ultimately, this approach would enhance the representativeness of the calibration process and improve the overall reliability of LCS-based air quality monitoring.

4. Conclusions

In the present study, hourly $PM_{2.5}$ measurements from LCSs installed at NARIT in Chiang Mai, Thailand, showed good agreement with those from reference-grade air quality monitor (PCD at 35T station) located 4 km away. The LCS $PM_{2.5}$ concentrations were likely overestimated during the dry season and underestimated during the rainy season. The effects of key environmental factors such as RH and temperature on the performance of LCS $PM_{2.5}$ concentration monitoring were investigated.

RH had significant nonlinear relationships with both the properties of the particles and the response of the LCSs. To address this, nonlinear regression approaches, specifically GAM and RF, were employed to calibrate the LCS $PM_{2.5}$ concentrations. Our study underscores the importance of including environmental and temporal factors in the GAM approach to enhance the accuracy of LCS $PM_{2.5}$ measurements. However, the GAM model in this study faced limitations in handling extremely high RH levels. Therefore, stratifying the dataset by season may offer a viable alternative to developing a more effective calibration algorithm for LCS $PM_{2.5}$ measurements. Extending the observation period will be essential to comprehensively understand the characteristics of seasonal $PM_{2.5}$ variation. The performance of the RF model was lower during extreme $PM_{2.5}$ events, suggesting its applicability could be compromised during periods of elevated $PM_{2.5}$ levels, such as those caused by agricultural burning during the dry season from February to April in Thailand. Despite this, we successfully demonstrated the value of employing a calibration method and confirmed that nonlinear regression approaches were more effective than conventional linear regression.

As LCSs hold promise for supporting regulatory air quality monitoring, especially for tracking 24-hour average $PM_{2.5}$ levels, further improvements in sensor accuracy,

environmental robustness, and validation will make them more fit for the task. Providing strong calibration methods to address environmental sensitivity could enable LCS networks to become valuable tools for air quality management; high-coverage real-time pollution monitoring could help public health policies provide timely interventions to protect community health.

In the future, we will assess LCS PM2.5 concentrations across different locations over extended periods to capture the full seasonal cycle of $PM_{2.5}$ pollution throughout Thailand. Moreover, further exploration of diverse calibration methods is needed to determine optimal solutions for calibrating LCS $PM_{2.5}$ concentrations under varying conditions, which should enhance the reliability and effectiveness of LCS-based monitoring in Thailand.

5. Acknowledgements

We gratefully acknowledge the Pollution Control Department of Thailand for providing the essential data used in this study. We also extend our sincere thanks to the National Astronomical Research Institute of Thailand (NARIT) for their support in supplying and maintaining the low-cost sensor (LCS) instruments, as well as for providing the corresponding data. Additionally, we are deeply appreciative of Chiang Mai University for awarding the CMU Presidential Scholarship, which supported this study. This research would not have been possible without the generous support and contributions from these institutions.

6. Conflicts of Interest

The authors declare that they have no conflicts of interest.

ORCID

Natthanidnan Sricharoen https://orcid.org/0009-0003-1743-5414

Titaporn Supasri https://orcid.org/0000-0003-3833-990X

Patrinee Traisathit https://orcid.org/0000-0003-2918-1928

Sukon Prasitwattanaseree https://orcid.org/0000-0002-1987-773X

Pimwarat Srikummoon https://orcid.org/0000-0003-1247-3131

References

Anderson, J. O., Thundiyil, J. G., & Stolbach, A. (2012). Clearing the air: A review of the effects of particulate matter air pollution on human health. *Journal of Medical Toxicology*, 8, 166-175. https://doi.org/10.1007/s13181-011-0203-1

Anik, M. T. H., Ebrahimabadi, M., Danger, J.-L., Guilley, S., & Karimi, N. (2021). Reducing aging impacts in digital sensors via run-time calibration. *Journal of Electronic Testing*, 37, 653-673. https://doi.org/10.1007/s10836-021-05976-8

Bai, L., Huang, L., Wang, Z., Ying, Q., Zheng, J., Shi, X., & Hu, J. (2020). Long-term field evaluation of low-cost particulate matter sensors in Nanjing. *Aerosol and Air Quality Research*, 20, 242-253. https://doi.org/10.4209/aaqr.2018.11.0424

Chantara, S., Thepnuan, D., Wiriya, W., Prawan, S., & Tsai, Y. I. (2019). Emissions of pollutant gases, fine particulate matters and their significant tracers from biomass

burning in an open-system combustion chamber. *Chemosphere,* 224, 407-416. https://doi.org/10.1016/j.chemosphere.2019.02.153

Chu, H.-J., Ali, M. Z., & He, Y.-C. (2020). Spatial calibration and $PM_{2.5}$ mapping of low-cost air quality sensors. *Scientifc Reports*, 10, Articl 22079. https://doi.org/10.1038/s41598-020-79064-w

Dejchanchaiwong, R., Tekasakul, P., Saejio, A., Limna, T., Le, T.-C., Tsai, C.-J., Lin, G.-Y., & Morris, J. (2023). Seasonal field calibration of low-cost $PM_{2.5}$ sensors in different locations with different sources in thailand. *Atmosphere,* 14(3), Article 496. https://doi.org/10.3390/atmos14030496

Eilers, P. H. C., & Marx, B. D. (1996). Flexible smoothing with B-splines and penalties. *Statistical Science*, 11(2), 89-121. https://doi.org/10.1214/ss/1038425655

Giordano, M. R., Malings, C., Pandis, S. N., Presto, A. A., McNeill, V. F., Westervelt, D. M., Beekmann, M., & Subramanian, R. (2021). From low-cost sensors to high-quality data: A summary of challenges and best practices for effectively calibrating low-cost particulate matter mass sensors. *Journal of Aerosol Science*, 158, Article 105833. https://doi.org/10.1016/j.jaerosci.2021.105833

Hagan, D. H., & Kroll, J. H. (2020). Assessing the accuracy of low-cost optical particle sensors using a physics-based approach. *Atmospheric Measurement Techniques*, 13(11), 6343-6355. https://doi.org/10.5194/amt-13-6343-2020

Hastie, T., & Tibshirani, R. (1986). Generalized additive models. *Statistical Science*, 1 (3), 297-318.

Hata, M., Chomanee, J., Thongyen, T., Bao, L., Tekasakul, S., Tekasakul, P., Otani, Y., & Furuuchi, M. (2014). Characteristics of nanoparticles emitted from burning of biomass fuels. *Journal of Environmental Sciences*, 26(9), 1913-1920. https://doi.org/10.1016/j.jes.2014.07.005

Hong, G.-H., Le, T.-C., Tu, J.-W., Chieh, W., Chang, S.-C., Yu, J.-Y., Lin, G.-Y., Aggarwal, S. G., & Tsai, C.-J. (2021). Long-term evaluation and calibration of three types of low-cost $PM_{2.5}$ sensors at different air quality monitoring stations. *Journal of Aerosol Science*, 157, Article 105829. https://doi.org/10.1016/j.jaerosci.2021.105829

Hua, J., Zhang, Y., de Foy, B, Mei, X., Shang, J., Zhang, Y., Sulaymon, I. D., & Zhou, D. (2021). Improved $PM_{2.5}$ concentration estimates from low-cost sensors using calibration models categorized by relative humidity. *Aerosol Science and Technology,* 55(5), 600-613. https://doi.org/10.1080/02786826.2021.1873911

Jain, S., Prestob, A. A., & Zimmerman, N. (2023). Using spatiotemporal prediction models to quantify $PM_{2.5}$ exposure due to daily movement. *Environmental Science: Atmospheres*, 3, 1665-1677. https://doi.org/10.1039/D3EA00051F

Jainontee, K., Pongkiatkul, P., Wang, Y. L., Weng, R. J. F., Lu, Y.-T., Wang, T.-S., & Chen, W.-K. (2023). Strategy design of $PM_{2.5}$ controlling for Northern Thailand. *Aerosol and Air Quality Research*, 23(6), Article 220432. https://doi.org/10.4209/aaqr.220432

Jayaratne, R., Liu, X., Thai, P., Dunbabin, M., & Morawska, L. (2018). The influence of humidity on the performance of a low-cost air particle mass sensor and the effect of atmospheric fog. *Atmospheric Measurement Techniques*, 11(8), 4883-4890. https://doi.org/10.5194/amt-11-4883-2018

Jayaratne, R., Liu, X., Ahn, K. H., Asumadu-Sakyi, A., Fisher, G., Gao, J., Mabon, A., Mazaheri, M., Mullins, B., Nyaku, M., Ristovski, Z., Scorgie, Y., Thai, P., Dunbabin, M., & Morawska, L. (2020). Low-cost $PM_{2.5}$ sensors: an assessment of their suitability for various applications. *Aerosol and Air Quality Research*, 20, 520-532. https://doi.org/10.4209/aaqr.2018.10.0390

Jon, K. S., Huang, Y.-D., Sin, C. H., Cui, P.-Y., & Luo, Y. (2023). Influence of wind direction on the ventilation and pollutant dispersion in different 3D street canyon configurations:

Numerical simulation and wind-tunnel experiment. *Environmental Science and Pollution Research*, 30, 31647-31675. https://doi.org/10.1007/s11356-022-24212-0

Lavanyaa, V. P., Varshini, S., Mitra, S. S., Hungund, K. M., Majumdar, R., & Srikanth, R. (2022). Geospatial modelling for estimation of $PM_{2.5}$ concentrations in two megacities in Peninsular India. *Aerosol and Air Quality Research*, 22(7), Article 220110. https://doi.org/10.4209/aaqr.220110

Lee, C.-H., Wang, Y.-B., & Yu, H.-L. (2019). An efficient spatiotemporal data calibration approach for the low-cost $PM_{2.5}$ sensing network: A case study in Taiwan. *Environment International*, 130, Article 104838. https://doi.org/10.1016/j.envint.2019.05.032

Lyu, B., Zhang, Y., & Hu, Y. (2017). Improving $PM_{2.5}$ air quality model forecasts in China using a bias-correction framework. *Atmosphere*, 8(8), Article 147. https://doi.org/10.3390/atmos8080147

Margaritis, D., Keramydas, C., Papachristos, I., & Lambropoulou, D. (2021). Calibration of low-cost gas sensors for air quality monitoring. *Aerosol and Air Quality Research*, 21(11), Article 210073. https://doi.org/10.4209/aaqr.210073

McFarlane, C., Raheja, G., Malings, C., Appoh, E. K. E., Hughes, A. F., & Westervelt, D. M. (2021). Application of gaussian mixture regression for the correction of low cost $PM_{2.5}$ monitoring data in Accra, Ghana. *ACS Earth and Space Chemistry*, 5(9), 2268-2279. https://doi.org/10.1021/acsearthspacechem.1c00217

Nalakurthi, N.V.S.R., Abimbola, I., Ahmed, T., Anton, I., Riaz, K., Ibrahim, Q., Banerjee, A., Tiwari, A., & Gharbia, S. (2024). Challenges and opportunities in calibrating low-cost environmental sensors. *Sensors*, 24(11), 3650. https://doi.org/10.3390/s24113650

Neal, L.S., Agnew, P., Moseley, S., Ordóñez, C., Savage, N. H., & Tilbee M. (2014). Application of a statistical post-processing technique to a gridded, operational, air quality forecast. *Atmospheric Environment*, 98, 385-393. https://doi.org/10.1016/j.atmosenv.2014.09.004

Noti, J. D., Blachere, F. M., McMillen, C. M., Lindsley, W. G., Kashon, M. L., Slaughter, D. R., & Beezhold, D. H. (2013). High humidity leads to loss of infectious influenza virus from simulated coughs. *PLoS ONE*, 8(2), e57485. https://doi.org/10.1371/journal.pone.0057485

Pani, S. K., Chantara, S., Khamkaew, C., Lee, C.-T., & Lin, N.-H. (2019). Biomass burning in the northern peninsular Southeast Asia: Aerosol chemical profile and potential exposure. *Atmospheric Research*, 224, 180-195. https://doi.org/10.1016/j.atmosres.2019.03.031

Park, D., Yoo, G.-W., Park, S.-H., & Lee, J.-H. (2021). Assessment and calibration of a low-cost $PM_{2.5}$ sensor using machine learning (HybridLSTM neural network): Feasibility study to build an air quality monitoring system. *Atmosphere*, 12(10), Article 1306. https://doi.org/10.3390/atmos12101306

Raheja, G., Nimo, J., Appoh, E. K.-E., Essien, B., Sunu, M., Nyante, J., Amegah, M., Quansah, R., Arku, R. E., Penn, S. L., Giordano, M. R., Zheng, Z., Jack, D., Chillrud, S., Amegah, K., Subramanian, R., Pinder, R., Appah-Sampong, E., Tetteh, E. N., Borketey, M. A., Hughes, A. F., & Westervelt, D. M. (2023). Low-cost sensor performance intercomparison, correction factor development, and 2+ years of ambient $PM_{2.5}$ monitoring in Accra, Ghana. *Environmental Science & Technology*, 57(29), 10708-10720. https://doi.org/10.1021/acs.est.2c09264

Raysoni, A. U., Sai, D. P., Mendez, E., Wladyka, D., Sepielak, K., & Temby, O. (2023). A review of literature on the usage of low-cost sensors to measure particulate matter. *Earth*, 4(1), 168-186. https://doi.org/10.3390/earth4010009

Salehi, M., Hashiani, A. A., Karimi, B., & Mirhoseini, S. H. (2023). Estimation of health-related and economic impacts of $PM_{2.5}$ in Arak, Iran, using BenMAP-CE. *PLoS ONE*, 18(12), Article e0295676. https://doi.org/10.1371/journal.pone.0295676

Salimifard, P., Rim, D., & Freihaut, J. D. (2019). Evaluation of low-cost optical particle counters for monitoring individual indoor aerosol sources. *Aerosol Science and Technology*, 54(2), 217-231. https://doi.org/10.1080/02786826.2019.1697423

Samae, H., Tekasakul, S., Tekasakul, P., & Furuuchi, M. (2021). Emission factors of ultrafine particulate matter (PM<0.1 μm) and particle-bound polycyclic aromatic hydrocarbons from biomass combustion for source apportionment. *Chemosphere*, 262, Article 127846. https://doi.org/10.1016/j.chemosphere.2020.127846

Sousan, S., Koehler, K., Thomas, G., Park, J. H., Hillman, M., Halterman, A., & Peters, T.M. (2016). Inter-comparison of low-cost sensors for measuring the mass concentration of occupational aerosols. *Aerosol Science and Technology*, 50(5), 462-473. https://doi.org/10.1080/02786826.2016.1162901

Srishti, S., Agrawal, P., Kulkarni, P., Gautam, H. C., Kushwaha, M., & Sreekanth, V. (2022). Multiple PM low-cost sensors, multiple seasons' data, and multiple calibration models. *Aerosol and Air Quality Research*, 23(3), Article 220428. https://doi.org/10.4209/aaqr.220428

Taimuri, B., Lakhani, S., Javed, M., Garg, D., Aggarwal, V., Mehndiratta, M. M., & Wasay, M. (2022). Air pollution and cerebrovascular disorders with special reference to asia: An overview. *Annals of Indian Academy of Neurology*, 25(Suppl 1), S3-S8. https://doi.org/10.4103/aian.aian_491_22

Thepnuan, D., Chantara, S., Lee, C.-T., Lin, N.-H., & Tsai, Y. I. (2019). Molecular markers for biomass burning associated with the characterization of $PM_{2.5}$ and component sources during dry season haze episodes in upper South East Asia. *Science of The Total Environment*, 658, 708-722. https://doi.org/10.1016/j.scitotenv.2018.12.201

Tomášková, H., Šlachtová, H., Dalecká, A., Polaufová, P., Michalík, J., Tomášek, I., & Šplíchalová, A. (2022). Association between $PM_{2.5}$ exposure and cardiovascular and respiratory hospital admissions using spatial GIS analysis. *Atmosphere*, 13(11), Article 1797. https://doi.org/10.3390/atmos13111797

Tsai, D.-R., Jhuang, J.-R., Su, S.-Y., Chiang, C.-J., Yang, Y.-W., & Lee, W.-C. (2022). A stabilized spatiotemporal kriging method for disease mapping and application to male oral cancer and female breast cancer in Taiwan. *BMC Medical Research Methodology*, 22(1), Article 270. https://doi.org/10.1186/s12874-022-01749-9

Vichit-Vadakan, N. & Vajanapoom, N. (2011). Health impact from air pollution in Thailand: Current and future challenges. *Environmental Health Perspectives*, 119(5), A197-A198. https://doi.org/10.1289/ehp.1103728

Wang, W.-C. V., Lung, S.-C. C., & Liu, C.-H. (2020). Application of machine learning for the in-field correction of a $PM_{2.5}$ low-cost sensor network. *Sensors*, 20(17), Article 5002. https://doi.org/10.3390/s20175002

Weisserta, L. F., Albertib, K., Miskella, G., Pattinsonc, W., Salmondd, J. A., Henshawb, G., & Williams, D. E. (2019). Low-cost sensors and microscale land use regression: Data fusion to resolve air quality variations with high spatial and temporal resolution. *Atmospheric Environment*, 213, 285-295. https://doi.org/10.1016/j.atmosenv.2019.06.019

World Health Organization. (2024, October 20). *Air pollution*. https://www.who.int/health-topics/ air-pollution#tab=tab_2

Yang, Z., Yang, J., Li, M., Chen, J., & Ou, C.-Q. (2021). Nonlinear and lagged meteorological effects on daily levels of ambient $PM_{2.5}$ and O_3: Evidence from 284 Chinese cities. *Journal of Cleaner Production*, 278, Article 123931. https://doi.org/10.1016/j.jclepro.2020.123931